

## SOLIDIFICATION AND MOULD-FLOW ANALYSIS OF THE CASTING OF GRIDS FOR LEAD/ACID BATTERIES

M. AOKI

*Shin-Kobe Electric Machinery Co. Ltd., Okabi-Machi Oka 2200, Oosato-gun, Saitama-ken (Japan)*

---

### Introduction

The grid of a lead/acid battery serves as a current collector, and its properties contribute greatly to the performance characteristics of the battery. Whereas one of the primary factors that determine the grid properties, namely, the alloy composition, has been studied extensively, there has been very little research on another important aspect, namely, the casting technology.

In recent times, progress has been made in computer technology for thermal analysis, with the result that it has become possible to use casting technology to control, to a certain extent, the properties of battery grids. This paper describes the determination of the heat-transfer coefficients during grid casting, together with measurements of flow and solidification of metal in the mould die.

### Experimental

#### *Determination of heat-transfer coefficients*

In order to apply computer technology to thermal analysis during grid casting, it is important to define the heat-transfer coefficient between the molten metal and the mould die. In the case of casting grids for lead/acid batteries, since cork is used for the releasing agent, it is necessary to determine the heat-transfer coefficient between both the molten metal and the cork, and between the cork and the mould die.

The above mentioned coefficients were obtained by measuring the temperatures of the molten metal and mould die at distances of 1.7, 4.2 and 6.0 mm from the interface between the metal and the mould, as shown in Fig. 1. The thickness of cork sprayed on the mould die was 0.07 mm and was measured with a depth-micrometer. The casting and mould-die temperatures were 480 °C and 150 °C, respectively. The cast material was a Pb-4 wt.%Sb alloy.

#### *Observation of mould flow*

One of the mould dies was constructed from transparent polymethyl methacrylate resin (Fig. 2), while the other was made from cast iron. Both dies had a 5 mm dia. grid for observation of the flow of molten metal.

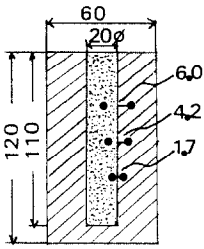


Fig. 1. Mould die used in analysis (dimensions in mm).

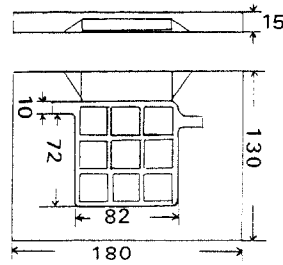


Fig. 2. Mould die (constructed from resin) used for observation of material flow (dimensions in mm).

In the case of the resin die, paraffin and mercury were poured and photographed. The temperature of the mould die was measured at several grid points by means of a thermocouple, a thermocouple signal transducer 12-bit A/D converter, and a personal computer. The data were gathered at  $5 \mu\text{s}$  intervals by 16-channel equipment.

#### *Alloy structure and corrosion test*

After polishing with  $0.06 \mu\text{m}$  alumina, the structure of the cast lead alloy was observed by scanning electron microscopy (SEM). The corrodibility of the alloy was examined after 240 h in 1.280 s.g.  $\text{H}_2\text{SO}_4$  at  $20^\circ\text{C}$  and a potentiostatically held voltage of 2.75 V. The morphology of the resulting corroded specimens was also examined by SEM.

## Results and discussion

### *Heat-transfer coefficient*

Values of the heat-transfer coefficient as a function of the cork thickness were determined by a curve-fitting method based on 2-dimensional differences in the thermal-analysis curve at each measurement point. The results are shown as curve B in Fig. 3.

Dividing the values on curve B by the thermal conductivity of the cork leads to curve A, also given in Fig. 3. Above a  $5 \times 10^{-3}$  cm thickness of cork, curve A shows relatively good agreement with curve B. Using the heat-transfer coefficient mentioned above, simulation of solidification without flow can be easily obtained.

### *Observation of mould flow*

The flow of molten paraffin and mercury in the polymethyl methacrylate die is shown in Fig. 4(A) and (B), respectively. The pattern of flow is very similar for both materials, and it can be seen that the materials fill from the bottom of the mould die, after flowing down directly from the gate.

(A) molten paraffin (B) mercury

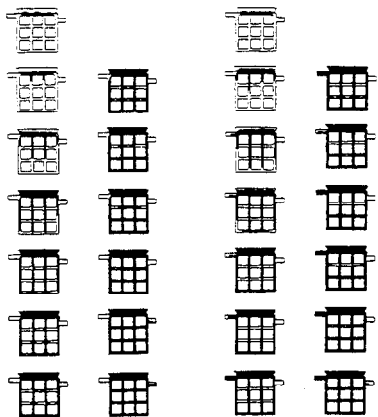
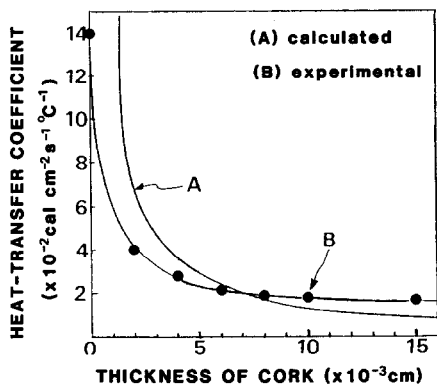


Fig. 3. Relationship between heat-transfer coefficient and cork thickness.

Fig. 4. States of flow.

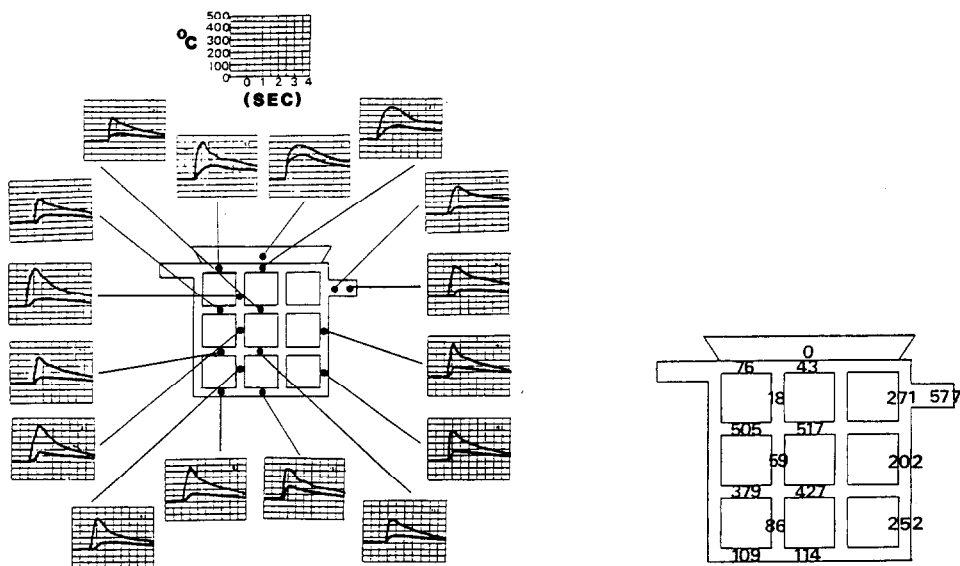


Fig. 5. Thermal-analysis data at various points in grid.

Fig. 6. Time (ms) for arrival of flow.

When lead alloy is poured into the metal die, thermal-analysis curves are required, as shown in Fig. 5. In this Figure, curve A represents the heat change at the centre of the grid and curve B represents the heat change at the interface between the grid and the cork. Using these curves, arrival times at each point from the centre of the grid can be obtained (Fig. 6). The time

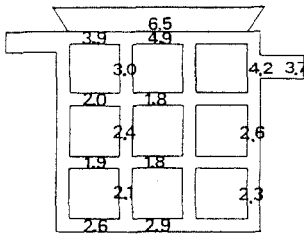


Fig. 7. Time interval (s) between arrival of flow and solidification.

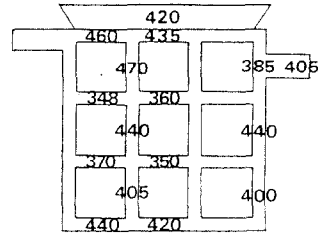


Fig. 8. Highest temperature ( $^{\circ}\text{C}$ ) at each measurement point in grid.

interval between arrival and solidification is shown in Fig. 7, and the highest temperature at each point in the mould is given in Fig. 8. From comparison of these results, it can be concluded that the flow of molten metal shown in Figs. 6 - 8 is very similar to the flow of molten lead. Incidentally, in the case of gravity casting, the flow of metal is considered to be a 'filling' of the mould die by lead, and not a flowing process. The results of a numerical analysis based on filling are compared with experimental data in Fig. 9. Good agreement between the two sets of data is obtained by assuming a filling speed of  $0.023 \text{ cm}^3 \text{ ms}^{-1}$ . Thus, it is confirmed that the arrival time at each point can be calculated from the filling speed.

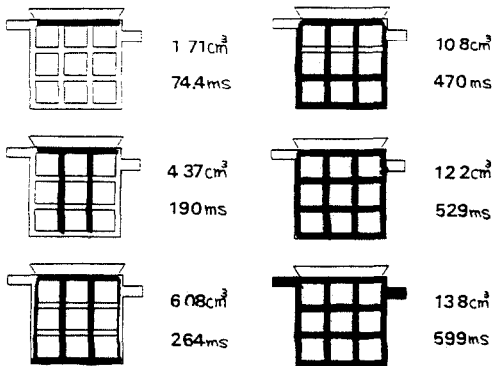


Fig. 9. States of filling: filling volume ( $\text{cm}^3$ ) and filling time (ms).

### *Alloy structure and corrosion rate*

The fresh and corroded structures of the metal are shown in Fig. 10. It can be seen that the structure and solidification at point A are very different to those at point B. The molten metal is poured to point A at high temperature and this takes a fairly long time, for point A is near to the gate. However, molten metal takes longer to reach point B at low temperature and therefore solidifies in a short time. Thus, the grain size of the structure at

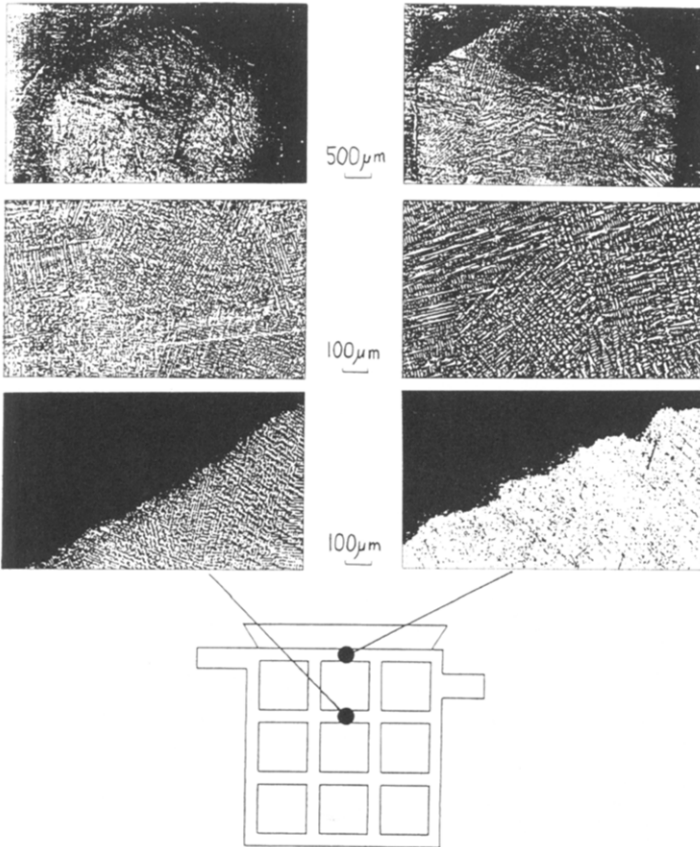


Fig. 10. Solidification structures and their corroded states.

point B is very small and the length of the secondary dendrite arm is about two-thirds that at point A. In addition, there are very few shrinkage cavities at point B.

These results can be explained by the cooling speed of the thermal analysis and the cooling effect at point B. The corrosion at point B is negligible. As mentioned above, the quality of the grid is controlled by the thermal conditions of the casting process. Both the control of the casting conditions and the simulation of flow and solidification on casting warrant further study.

## Conclusions

(i) From determination of the heat-transfer coefficient during grid casting, solidification analysis has become possible.

(ii) Metal flow in the mould has been observed, and it has been found that the heat conditions due to the flow cause marked changes in the grid properties.

### **Bibliography**

- 1 I. Onaka, *An Introduction to Heat Transfer and Coagulation Analysis by Computer*, Maruzen, 1985.
- 2 E. Niyama, *Imono*, 42 (1970) 1006.